A New Synthetic Route to W≡W and Mo≡W Compounds of the Type $MM'X_4(PR_3)_4$, X = Cl or Br. Structural Characterization of $W_2WBr_4(\mu\text{-dppm})_2$ and $Mo_2WBr_4(PMe_2Ph)_4$ and $^{31}P\{^1H\}$ NMR Spectra of These and Related Compounds

F. A. Cotton,* Judith L. Eglin,† and Chris A. James‡

Department of Chemistry and Laboratory for Molecular Structure and Bonding, Texas A&M University, College Station, Texas 77843

Received August 12, 1992

A new synthetic route that is more convenient and more general than any previously available has now been developed for quadruply bonded W_2^{4+} compounds. This new synthetic route has been used in the preparation of complex **1**, $W_2WBr_4(\mu\text{-dppm})_2$, and in addition two known ditungsten compounds, $W_2Cl_4(PMe_3)_4$ (**3**) and $W_2Cl_4(PMe_2Ph)_4$ (**4**). The quadruply bonded complexes **1** and $Mo_2WBr_4(PMe_2Ph)_4$ (**2**) are formed in the reactions between WBr_5 and bis(diphenylphosphino)methane and $WBr_4(PPh_3)_2$ and $Mo(\eta^6\text{-}C_6H_5PMe_2)(PMe_2Ph)_3$, respectively. These are the only examples of quadruply bonded complexes that contain either a W_2WBr_4 or Mo_2WBr_4 core. The W≡W and apparent Mo≡W distances for $W_2WBr_4(\mu\text{-dppm})_2$ and $Mo_2WBr_4(PMe_2Ph)_4$ are 2.2632(9) and 2.209(1) Å, respectively. Complex **2** is contaminated by small amounts of the dimolybdenum analog. In addition to the structural data for these complexes, each has been fully characterized using $^{31}P\{^1H\}$ NMR and UV–vis spectroscopy. Preliminary spectroscopic data have been obtained for $W_2WBr_4(PMe_2Ph)_4$ (**5**), $W_2WBr_4(PPh_2Me)_4$ (**6**), and $Mo_2WBr_4(PPh_2Me)_4$ (**7**). Complex **1** has methylene protons located at positions that allow the calculation of the diamagnetic anisotropy of the W≡W bond from the ^1H NMR chemical shift data. The diamagnetic anisotropy for the W≡W bond in $W_2WBr_4(\mu\text{-dppm})_2$ has been estimated and will be compared to the diamagnetic anisotropy estimated for $W_2WCl_4(\mu\text{-dppm})_2$ and $\alpha\text{-}W_2WCl_4(dppe)_2$. The crystal structures of **1** and **2** are fully described. Crystallographic data for these compounds are as follows: compound **1**, $P2_1$ with a = 10.047(1) Å, b = 14.529(2) Å, c = 23.668(3) Å, β = 95.294(1)°, V = 3440(1) Å^3, and Z = 2; compound **2**, $Fdd2$ with a = 18.313(4) Å, b = 43.981(7) Å, c = 9.570(2) Å, V = 7709(2) Å^3, and Z = 8.

Introduction

Ditungsten complexes that contain a W≡W bond are difficult to synthesize and manipulate, whereas, in contrast, there are many quadruply bonded dimolybdenum complexes that contain various ligand types.[1] This is due, in part, to the presence of a weak δ bond and the greater sensitivity of the tungsten compounds to oxygen. However, it is also due to the lack of a good starting material or a convenient preparative route. The use of Me_3SiX reagents (X = Cl, Br, I and SCN) has allowed a variety of $Mo_2X_4L_4$ and $Mo_2X_4(L\text{-}L)_2$ complexes (L = monodentate phosphine ligand and L-L = bidentate phosphine ligand) to be synthesized from $Mo_2Mo(O_2CCMe_3)_4$ and $Mo_2Mo(O_2CCF_3)_4$.[2-4] In contrast, $W_2W(O_2CCF_3)_4$ is very sensitive to oxygen, and the analogous synthetic routes are thus not available in ditungsten chemistry. Since WCl_4 has been the tungsten starting material for complexes of the general type $W_2WX_4L_4$, the halide, X, has been chloride for all compounds prepared to date. Compounds with bidentate phosphine ligands, $W_2WCl_4(L\text{-}L)_2$, have usually been synthesized via phosphine substitution reactions on monophosphine precursors.[5-7] The use of $NaBEt_3H$ as a reducing agent allows the convenient synthesis of $W_2WX_4L_4$ and $W_2WX_4(L\text{-}L)_2$, X = Cl or Br, complexes in good yield in several solvents with a variety of reaction conditions.

Limitations similar to those which exist for the ditungsten systems are also encountered for the Mo≡W systems. A facile synthetic route for the formation of $Mo_2WCl_4L_4$ type complexes was reported by Luck and Morris in 1984.[8] An extension of this preparative method has been employed to synthesize $Mo_2WBr_4L_4$ type complexes.

Experimental Section

General Data. All manipulations were carried out under an atmosphere of argon unless otherwise specified. Standard Schlenk and vacuum line techniques were used. Commercial grade solvents, except alcohols and dichloro- and dibromomethane, were dried over and freshly distilled from potassium/sodium benzophenone ketyl prior to use. Alcohols and dichloro- and dibromomethane were dried over magnesium alkoxides and phosphorus pentoxide respectively and freshly distilled prior to use. $Mo(\eta^6\text{-}C_6H_5PMe_2)(PMe_2Ph)_3$ and $Mo(\eta^6\text{-}C_6H_5PMePh)(PMePh_2)_3$ were prepared as described in the literature[9,10] and $WBr_4(PPh_3)_2$ (**8**) was prepared by a procedure, similar to the preparation of $WCl_4(PPh_3)_2$, that is described in detail here.[11] The compounds $W_2WCl_4(Ph_2Me)_4$,[6] $W_2WCl_4(\mu\text{-dppm})_2$,[5] $\alpha\text{-}W_2WCl_4(dppe)_2$,[6] $Mo_2MoCl_4(\mu\text{-dppm})_2$,[2] $Mo_2MoBr_4(\mu\text{-dppm})_2$,[12] and $Mo_2MoI_4(\mu\text{-dppm})_2$[4] used in the spectroscopic studies were prepared by literature methods. The phosphines were purchased from Strem Chemicals and dried in vacuum prior to use. $NaBEt_3H$ was purchased from Aldrich as a 1 M solution in toluene. The visible spectra were recorded on a Cary 17D spectrophotometer. The

† Present address: Mississippi State University, Mississippi State, MS 39762.

‡ Present address: Los Alamos National Laboratory, INC-14 Los Alamos, NM 87545.

(1) Cotton, F. A.; Walton, R. A. *Multiple Bonds Between Metal Atoms*, 2nd ed.; Oxford Univ. Press: London, 1993.
(2) Agaskar, P. A.; Cotton, F. A. *Inorg. Chem.* **1984**, *23*, 3383.
(3) Agaskar, P. A.; Cotton, F. A.; Derringer, D. R.; Powell, G. L.; Root, D. R.; Smith, T. J. *Inorg. Chem.* **1985**, *24*, 2786.
(4) Cotton, F. A.; Dunbar, K. R.; Poli, R. *Inorg. Chem.* **1986**, *25*, 3700.
(5) Canich, J. A. M.; Cotton, F. A. *Inorg. Chim. Acta* **1988**, *142*, 69.
(6) Schrock, R. R.; Sturgeoff, L. G.; Sharp, P. R. *Inorg. Chem.* **1983**, *22*, 2801.
(7) Schrock, R. R.; Sharp, P. R. *J. Am. Chem. Soc.* **1983**, *102*, 1430.
(8) Luck, R. L.; Morris, R. H.; Sawyer, J. F. *Inorg. Chem.* **1987**, *26*, 2422.
(9) Cotton, F. A.; Luck, R. L.; Morris, R. H. *Organometallics* **1989**, *8*, 1282.
(10) Luck, R. L.; Morris, R. H.; Sawyer, J. F. *Organometallics* **1984**, *3*, 247.
(11) Butcher, A. V.; Chatt, J.; Leigh, G. J.; Richards, R. L. *J. Chem. Soc., Dalton Trans.* **1972**, 1064.
(12) Best, S. A.; Smith, T. J.; Walton, R. A. *Inorg. Chem.* **1978**, *17*, 99.

0020-1669/93/1332-0681$04.00/0

$^{31}P\{^1H\}$ NMR (81 MHz) and ^1H NMR (200 MHz) spectra were recorded on a Varian XL-200 spectrometer. The $^{31}P\{^1H\}$ NMR chemical shift values were referenced externally and are reported relative to 85% H_3PO_4.

Preparation of $W_2^{4+}WBr_4(\mu\text{-dppm})_2$ (1). To a red solution of 0.400 g (0.69 mmol) of WBr_5 dissolved in 10 mL of toluene, 2.1 mL (2.1 mmol) of a 1 M solution of $NaBEt_3H$ was added. After the solution was stirred for approximately 30 min, a solution of 0.400 g (1.04 mmol) of dppm (bis(diphenylphosphino)methane) in 20 mL of toluene was added. The mixture was stirred overnight to ensure completion of the reaction. All solvent was removed in vacuum, the precipitate dissolved in benzene, and the solution filtered through Celite. Addition of hexanes produced a brown/green precipitate, which was washed with hexanes and then methanol and dried in vacuum (205 mg, 41%).

Preparation of $W_2^{4+}WCl_4(PMe_3)_4$ (3) and $W_2^{4+}WCl_4(PMe_2Ph)_4$ (4). To 0.200 g (0.61 mmol) of WCl_4 was added 10 mL of THF. The solution was cooled to −60 °C, and 1.22 mL (1.22 mmol) of a 1 M solution of $NaBEt_3H$ in toluene was added, causing the solution to become green/brown in color. After the mixture was stirred for approximately 20 min, 2.44 mmol of either PMe_3 or PMe_2Ph was added. The reaction mixture became a deep forest green color at low temperature and was allowed to warm to room temperature slowly (0.5 h). After the mixture was stirred at room temperature for 12 h to ensure completion of the reaction, all solvent was removed. The resultant green powder was dissolved in THF, filtered through Celite, and precipitated with hexanes. The green precipitate was washed with hexanes and then methanol and dried in vacuum. (154 mg, 63% $W_2^{4+}WCl_4(PMe_3)_4$, or 248 mg, 76% $W_2^{4+}WCl_4(PMe_2Ph)_4$. The identity of the products was confirmed by $^{31}P\{^1H\}$ NMR spectroscopy.

Preparation of $W_2^{4+}WBr_4(PMe_2Ph)_4$ (5) and $W_2^{4+}WBr_4(PPh_2Me)_4$ (6). To 0.200 g (0.34 mmol) of WBr_5 was added 10 mL of THF. The deep red solution was cooled to −60 °C, and 1.02 mL (1.02 mmol) of a 1 M solution of $NaBEt_3H$ in toluene was added, causing the solution to become grey/brown in color. After the mixture was stirred for approximately 20 min, 1.37 mmol of either PMe_2Ph or PPh_2Me was added. The reaction mixture became a deep green/brown color and was allowed to warm slowly to room temperature (0.5 h). After the mixture was stirred for 12 h to ensure completion of the reaction, all solvent was removed in vacuum. The precipitate was dissolved in THF, filtered through Celite, and precipitated with hexanes. The green/brown product was washed with hexanes and then methanol and dried in vacuum. The identity of the products was confirmed by $^{31}P\{^1H\}$ NMR and UV–vis spectroscopy. No attempts were made to optimize the yields in these reactions.

Preparation of $Mo_2^{4+}WBr_4(PMe_2Ph)_4$ (2). A solution of $Mo(\eta^6\text{-}C_6H_5PMe_2)(PMe_2Ph)_3$ (0.100 g, 0.2 mmol) in 10 mL of benzene was added to a stirred slurry of $WBr_4(PPh_3)_2$ (0.412 g, 0.4 mmol) in 10 mL of benzene. After the mixture was stirred for 2 h, the green solution of **2** was filtered through Celite. The solution was concentrated to 3 mL, and 10 mL of methanol was added to cause precipitation. The green precipitate was then filtered, washed with methanol, and dried in vacuum (0.180 g, 78%).

Preparation of $Mo_2^{4+}WBr_4(PPh_2Me)_4$ (7). A solution of $Mo(\eta^6\text{-}C_6H_5PMePh)(PMePh_2)_3$ (0.179 g, 0.2 mmol) in 10 mL of benzene was added to a stirred slurry of $WBr_4(PPh_3)_2$ (0.412 g, 0.4 mmol) in 10 mL benzene. Stirring was continued for 2 h and the slurry then filtered through Celite to yield a green/brown solution of complex **7**. The solution was concentrated to 3 mL, and 10 mL of methanol was added to cause precipitation. The green precipitate was filtered, washed with methanol, and dried in vacuum. The identity of the product was confirmed by $^{31}P\{^1H\}$ NMR and UV–vis spectroscopy. No attempts were made to optimize the yields in this reaction.

Preparation of $WBr_4(PPh_3)_2$ (8). To 6.0 g (10.3 mmol) of WBr_5 dissolved in 40 mL of dibromomethane was added 6.12 g of zinc. After the mixture was stirred for 10 min, 50 g (190 mmol) of PPh_3 was added. The solution turned orange in color, and a bright orange precipitate formed. After this was stirred for an additional 10 min, 10 mL of benzene was added to ensure complete precipitation of the product, $WBr_4(PPh_3)_2$. The orange precipitate was then filtered, washed with copious amounts of benzene and hexanes and dried in vacuum (6.5 g, 61%).

X-ray Crystallography

Single-crystal diffraction experiments were conducted using a P3 automated diffractometer with Mo Kα radiation for **1** and **2**. Routine unit cell identification and intensity data collection procedures were followed utilizing the options specified in Table I and the general procedures previously described.[13] Lattice dimensions and Laue symmetry were verified using axial photographs. Three standard reflections were measured every hour during data collections to monitor any gain or loss in intensity and a correction applied when ΔI was greater than 3%. Corrections for Lorentz, polarization, and absorption effects were applied to both data sets. The latter correction was based on azimuthal scans of several reflections with diffractometer angle χ near 90°.[14]

Table I. Crystallographic Data and Data Collection Parameters for $W_2^{4+}WBr_4(\mu\text{-dppm})_2$ and $Mo_2^{4+}WBr_4(PMe_2Ph)_4$

	1	2
chem formula	$W_2Br_4P_4C_{50}C_{50}H_{44}$	$WMoBr_4P_4C_{32}H_{44}$
fw	1729.66	1152.03
space group (No.)	$P2_1$ (4)	$Fdd2$ (43)
a, Å	10.047(1)	18.313(4)
b, Å	14.529(2)	43.981(7)
c, Å	23.668(3)	9.570(2)
α, deg	(90)	(90)
β, deg	95.294(2)	(90)
γ, deg	(90)	(90)
V, Å^3	3440(1)	7709(2)
Z	2	8
T, °C	23 ± 2	23 ± 2
λ, Å	0.710 73	0.710 73
ρ_{calcd}, g cm^{-3}	1.719	1.985
μ(Mo Kα), cm^{-1}	58.475	76.596
transm coeff	0.9994–0.6804	0.9986–0.5334
R,[a] R_w[b]	0.0409, 0.044	0.0467, 0.0558

[a] $R = \sum||F_o| - |F_d||/\sum|F_o|$. [b] $R_w = [\sum w(|F_o| - |F_c|)^2/\sum w|F_o|^2]^{1/2}$; $w = 1/\sigma^2(|F_o|)$.

General Structure Solution and Refinement. The following general procedures were employed for the solution and refinement of both structures unless otherwise noted.

The heavy-atom positions were obtained from three dimensional Patterson functions. The positions for the remainder of the non-hydrogen atoms were found using a series of full matrix refinements followed by difference Fourier syntheses. These positions were initially refined with isotropic thermal parameters, then with anisotropic thermal parameters to convergence. The phenyl groups were refined as rigid bodies geometrically idealized as hexagons with C–C = 1.395 Å and C–H = 0.98 Å. However, each C atom was permitted to have a freely varying anisotropic displacement tensor. The hydrogen atoms, where included, were placed and fixed at calculated positions and their isotropic thermal parameters constrained to one variable, and the entire model was refined to convergence. Final refinements employed the SHELX-76 package of programs with variations in occupancy factors used to determine the composition of the metal atom sites in **2**. Important details pertinent to individual compounds are presented in Table I and in the following paragraphs.

Compound 1. Block shaped single crystals of **1** were obtained by placing a layer of methanol over a benzene solution of $W_2^{4+}WBr_4(dppm)_2$ (1:8) in long glass tubes sealed under an argon atmosphere. One of these crystals was sealed in a capillary.

Systemic absences narrowed the choice of space groups to $P2_1$ or $P2_1/m$. Initial refinements in $P2_1/m$, which requires the molecule to have mirror symmetry, resulted in high thermal parameters for the Br, P, and C atoms. Subsequent refinement in $P2_1$ resulted in lower thermal parameters and revealed the presence of a slight twist (3–4°) between the two ends of the molecule. These factors indicated that $P2_1$ was the proper space group. The final difference Fourier map contained several small "ghost" peaks in close proximity to the heavy atoms positions but no effort was made to correct for this problem. The final refinement factors after convergence are listed in Table I. Table II contains positional and thermal parameters. Selected bond distances and angles are given in Table III, and an ORTEP drawing of the core is shown in Figure 1.

Compound 2. Block shaped single crystals of **2** were obtained by placing a mixture of toluene and methanol (1:4) in long glass tubes sealed under an argon atmosphere and keeping these tubes in a refrigerator at −20 °C for several weeks. One of these crystals was coated with a thin layer of epoxy cement and mounted on the tip of a quartz fiber.

Systemic absences uniquely determined the space group as $Fdd2$. Hybrid atoms (MW) composed of 50% Mo and 50% W were placed at

(13) Bino, A.; Cotton, F. A.; Fanwick, P. E. *Inorg. Chem.* **1979**, *18*, 3558.
(14) North, A. C. T.; Phillips, D. A.; Matthews, F. S. *Acta Crystallogr., Sect. A.: Cryst. Phys., Diffr., Theor. Gen. Crystallogr.* **1968**, *24A*, 351.

Table II. Positional and Thermal Parameters for Non-Hydrogen Atoms of $W\equiv WBr_4(\mu\text{-dppm})_2$.

atom	x	y	z	B,[a] Å^2	atom	x	y	z	B,[a] Å^2
W(1)	0.20701(7)	0.17237(0)	0.24757(3)	2.61(2)	C(123)	0.138(1)	0.1012(8)	0.5035(5)	6.5(2)
W(2)	0.21908(8)	0.32778(6)	0.25208(3)	2.62(2)	C(124)	0.269(1)	0.1303(8)	0.5192(5)	7.2(2)
Br(1)	0.4137(3)	0.1071(2)	0.3002(1)	4.72(7)	C(125)	0.345(1)	0.1693(8)	0.4788(5)	7.8(2)
Br(2)	−0.0186(3)	0.1411(2)	0.1955(1)	4.25(6)	C(126)	0.290(1)	0.1791(8)	0.4228(5)	4.3(2)
Br(3)	0.4446(3)	0.3613(2)	0.3037(1)	4.25(6)	C(204)	0.455(2)	0.254(2)	0.1602(7)	3.1(2)
Br(4)	0.0124(3)	0.3952(2)	0.1989(1)	4.59(7)	C(211)	0.463(1)	0.0531(7)	0.1676(5)	2.5(2)
P(1)	0.0785(6)	0.1589(4)	0.3345(3)	2.8(1)	C(212)	0.600(1)	0.0620(7)	0.1627(5)	5.7(2)
P(2)	0.3455(6)	0.1484(4)	0.1619(3)	2.7(1)	C(213)	0.681(1)	−0.0160(7)	0.1648(5)	5.7(2)
P(3)	0.0827(7)	0.3611(4)	0.3379(3)	3.3(1)	C(214)	0.626(1)	−0.1028(7)	0.1719(5)	6.5(2)
P(4)	0.3432(6)	0.3510(4)	0.1656(3)	3.0(1)	C(215)	0.489(1)	−0.1117(7)	0.1768(5)	7.9(2)
C(1)	0.481(1)	0.772(1)	0.3719(6)	8.7(2)	C(216)	0.408(1)	−0.0337(7)	0.1747(5)	5.9(2)
C(2)	0.451(1)	0.680(1)	0.3591(6)	8.2(2)	C(221)	0.277(1)	0.1285(8)	0.0886(5)	3.8(2)
C(3)	0.356(1)	0.658(1)	0.3144(6)	10.5(3)	C(222)	0.350(1)	0.1510(8)	0.0434(5)	4.9(2)
C(4)	0.291(1)	0.728(1)	0.2825(6)	18.9(3)	C(223)	0.300(1)	0.1312(8)	−0.0121(5)	8.1(2)
C(5)	0.320(1)	0.820(1)	0.2952(6)	30.9(2)	C(224)	0.175(1)	0.0889(8)	−0.0225(5)	6.6(2)
C(6)	0.415(1)	0.842(1)	0.3399(6)	12.8(3)	C(225)	0.101(1)	0.0665(8)	0.0227(5)	6.5(2)
C(51)	0.328(1)	0.749(2)	0.5765(7)	17.5(3)	C(226)	0.152(1)	0.0862(8)	0.0782(5)	5.0(2)
C(52)	0.278(1)	0.674(2)	0.5440(7)	10.7(3)	C(311)	−0.035(1)	0.4592(7)	0.3320(5)	3.7(2)
C(53)	0.226(1)	0.688(2)	0.4879(7)	11.9(3)	C(312)	0.021(1)	0.5457(7)	0.3428(5)	4.2(2)
C(54)	0.224(1)	0.776(2)	0.4642(7)	11.5(3)	C(313)	−0.059(1)	0.6242(7)	0.3388(5)	5.8(2)
C(55)	0.274(1)	0.850(2)	0.4967(7)	9.1(3)	C(314)	−0.196(1)	0.6162(7)	0.3239(5)	5.3(2)
C(56)	0.326(1)	0.837(2)	0.5529(7)	12.0(3)	C(315)	−0.253(1)	0.5296(7)	0.3131(5)	5.6(2)
C(61)	0.274(1)	0.832(1)	−0.0416(5)	9.6(2)	C(316)	−0.173(1)	0.4511(7)	0.3171(5)	3.8(2)
C(62)	0.232(1)	0.749(1)	−0.0660(5)	11.6(2)	C(321)	0.149(1)	0.3772(8)	0.4122(5)	3.7(2)
C(63)	0.267(1)	0.666(1)	−0.0385(5)	13.2(3)	C(322)	0.069(1)	0.3614(8)	0.4563(5)	6.5(2)
C(64)	0.345(1)	0.667(1)	0.0134(5)	11.9(3)	C(323)	0.117(1)	0.3816(8)	0.5121(5)	5.1(2)
C(65)	0.388(1)	0.751(1)	0.0378(5)	10.0(2)	C(324)	0.246(1)	0.4178(8)	0.5238(5)	6.2(2)
C(66)	0.352(1)	0.833(1)	0.0103(5)	9.0(2)	C(325)	0.326(1)	0.4336(8)	0.4797(5)	10.3(2)
C(71)	0.003(1)	0.327(1)	0.8159(5)	16.8(2)	C(326)	0.278(1)	0.4134(8)	0.4239(5)	6.2(2)
C(72)	0.009(1)	0.181(1)	0.8194(5)	11.6(2)	C(411)	0.4556(9)	0.4507(7)	0.1707(5)	4.2(2)
C(73)	0.035(1)	0.259(1)	0.8045(5)	10.1(3)	C(412)	0.3971(9)	0.5374(7)	0.1741(5)	5.5(2)
C(103)	−0.024(2)	0.260(2)	0.3375(7)	3.2(2)	C(413)	0.4763(9)	0.6163(7)	0.1749(5)	7.4(2)
C(111)	−0.028(1)	0.0622(8)	0.3286(5)	3.3(2)	C(414)	0.6140(9)	0.6086(7)	0.1723(5)	4.9(2)
C(112)	0.035(1)	−0.0231(8)	0.3363(5)	3.9(2)	C(415)	0.6725(9)	0.5220(7)	0.1689(5)	4.9(2)
C(113)	−0.042(1)	−0.1034(8)	0.3352(5)	6.6(2)	C(416)	0.5933(9)	0.4430(7)	0.1681(5)	3.0(2)
C(114)	−0.181(1)	−0.0984(8)	0.3264(5)	8.1(2)	C(421)	0.269(1)	0.3654(8)	0.0927(4)	3.0(2)
C(115)	−0.243(1)	−0.0131(8)	0.3187(5)	4.6(2)	C(422)	0.144(1)	0.3279(8)	0.0765(4)	4.6(2)
C(116)	−0.167(1)	0.0673(8)	0.3198(5)	5.2(2)	C(423)	0.094(1)	0.3282(8)	0.0196(4)	4.8(2)
C(121)	0.159(1)	0.1499(8)	0.4071(5)	3.6(2)	C(424)	0.169(1)	0.3661(8)	−0.0213(4)	5.5(2)
C(122)	0.084(1)	0.1110(8)	0.4475(5)	4.6(2)	C(425)	0.295(1)	0.4036(8)	−0.0051(4)	6.0(2)
C(426)	0.345(1)	0.4033(8)	0.0519(4)	4.5(2)					

[a] Anisotropically refined atoms are given in the form of the equivalent isotropic displacement parameter defined as $^1/_3[a^2a^{*2}B_{11} + b^2b^{*2}B_{22} + c^2c^{*2}B_{33} + 2ab(\cos\gamma)a^*b^*B_{12} + 2ac(\cos\beta)a^*c^*B_{13} + 2bc(\cos\alpha)b^*c^*B_{23}]$.

the metal atom positions in the initial stages of the refinement, but this 1:1 constraint was later lifted. The final difference Fourier contained several small "ghost" peaks in close proximity to the heavy atoms, but no effort was made to correct for this problem. The composition of the hybrid metal atom, 53.8(7)% Mo and 46.2(7)% W, in the final refinement is in reasonable agreement with the $^{31}P\{^1H\}$ NMR spectrum of a solution of the crystals, which indicated the presence of ca. 5% $Mo\equiv MoBr_4(PMe_2Ph)_4$. The final refinement factors after convergence are listed in Table I. Table IV contains positional and thermal parameters. Selected bond distances and angles are given in Table V, and an ORTEP drawing is shown in Figure 2.

Results and Discussion

Syntheses. Synthesis of $W\equiv WBr_4(\mu\text{-dppm})_2$ (1). The synthesis of $W\equiv WBr_4(\mu\text{-dppm})_2$ is straightforward and proceeds in toluene at room temperature. Prior to this, all reported preparations were done in THF at low temperature, and only one other quadruply bonded ditungsten complex with bidentate phosphine ligands had been synthesized in a one-step preparation.[1,5-7,15] The use of $NaBEt_3H$ to reduce W(V) to W(II) is a clean, relatively fast procedure since the reaction mixture is homogeneous, unlike the reaction with Na/Hg as the reducing agent. Since boranes and NaX where X = Cl or Br are the byproducts of the reaction, the product does not have to be soluble in the reaction mixture in order to allow easy separation as in the case where Na/Hg is the reducing agent. $NaBEt_3H$ is commercially available as a 1 M solution in a variety of solvents and is easy to measure and transfer.

The use of $NaBEt_3H$ at room temperature in toluene is a general synthetic route and can be used in the direct synthesis of $W\equiv W$ complexes with either monodentate or bidentate phosphine ligands. In contrast, attempts to synthesize $W\equiv WBr_4(\mu\text{-dppm})_2$ directly in THF at −60 °C failed, although the syntheses of $W_2X_4L_4$ where L = PMe_3, PMe_2Ph, or PPh_2Me and X = Cl or Br proceed in both toluene at room temperature and THF at −60 °C. Since the synthesis of quadruply bonded ditungsten compounds proceeds straightforwardly in toluene, the thermally sensitive intermediate $Na_4(THF)_xW_2Cl_8$ is not the only pathway available in the synthesis of these compounds.[16]

The low temperature syntheses in THF that have been used to prepare **3**–**6** are similar to the preparative route of Schrock, except for the change in the reducing agent from Na/Hg to $NaBEt_3H$, but it is much easier to isolate the final product since the reaction mixture does not have to be separated from amalgam.[6] Neither Na/Hg nor hydrides other than $NaBEt_3H$ have been investigated as reducing agents at room temperature in toluene. The use of other solvents, such as benzene, with $NaBEt_3H$ as the reducing agent in the preparation of these compounds has also not yet been attempted.

The major difference between the syntheses of the $W\equiv WBr_4$ and the $W\equiv WCl_4$ cores is the starting material,

(15) Fryzuk, M. D.; Kreiter, C. G.; Sheldrick, W. S. *Chem. Ber.* **1989**, *122*, 851.

(16) Cotton, F. A.; Mott, G. N. *J. Am. Chem. Soc.* **1982**, *104*, 6781.

Table III. Selected Bond Lengths (Å) and Angles (deg) for $W\equiv WBr_4(\mu\text{-dppm})_2$[a]

Bond Lengths			
W(1)–W(2)	2.2632(9)	P(1)–C(121)	1.84(1)
W(1)–Br(1)	2.507(3)	P(2)–C(204)	1.89(2)
W(1)–Br(2)	2.520(3)	P(2)–C(211)	1.82(1)
W(1)–P(1)	2.535(6)	P(2)–C(221)	1.83(1)
W(1)–P(2)	2.586(6)	P(3)–C(103)	1.82(2)
W(2)–Br(3)	2.521(3)	P(3)–C(311)	1.85(1)
W(2)–Br(4)	2.524(3)	P(3)–C(321)	1.84(1)
W(2)–P(3)	2.598(7)	P(4)–C(204)	1.82(2)
W(2)–P(4)	2.516(6)	P(4)–C(411)	1.83(1)
P(1)–C(103)	1.80(2)	P(4)–C(421)	1.83(1)
P(1)–C(111)	1.76(1)		
Bond Angles			
W(2)–W(1)–Br(1)	108.39(7)	W(1)–P(1)–C(121)	123.4(4)
W(2)–W(1)–Br(2)	104.19(7)	C(103)–P(1)–C(111)	107.9(7)
W(2)–W(1)–P(1)	93.9(1)	C(103)–P(1)–C(121)	103.1(7)
W(2)–W(1)–P(2)	98.1(1)	C(111)–P(1)–C(121)	103.3(6)
Br(1)–W(1)–Br(2)	147.28(9)	W(1)–P(2)–C(204)	105.3(6)
Br(1)–W(1)–P(1)	91.6(1)	W(1)–P(2)–C(211)	115.9(4)
Br(1)–W(1)–P(2)	81.8(1)	W(1)–P(2)–C(221)	125.5(5)
Br(2)–W(1)–P(1)	83.1(1)	C(204)–P(2)–C(211)	104.1(7)
Br(2)–W(1)–P(2)	96.7(1)	C(204)–P(2)–C(221)	106.1(7)
P(1)–W(1)–P(2)	167.7(2)	C(211)–P(2)–C(221)	97.9(6)
W(1)–W(2)–Br(3)	104.90(7)	W(2)–P(3)–C(103)	101.6(6)
W(1)–W(2)–Br(4)	109.00(7)	W(2)–P(3)–C(311)	117.7(5)
W(1)–W(2)–P(3)	101.1(1)	W(2)–P(3)–C(321)	126.8(5)
W(1)–W(2)–P(4)	97.1(1)	C(103)–P(3)–C(311)	104.2(7)
Br(3)–W(2)–Br(4)	145.9(1)	C(103)–P(3)–C(321)	105.7(7)
Br(3)–W(2)–P(3)	95.8(2)	C(311)–P(3)–C(321)	98.5(6)
Br(3)–W(2)–P(4)	83.0(1)	W(2)–P(4)–C(204)	108.0(6)
Br(4)–W(2)–P(3)	81.3(2)	W(2)–P(4)–C(411)	113.6(5)
Br(4)–W(2)–P(4)	89.4(2)	W(2)–P(4)–C(421)	126.5(4)
P(3)–W(2)–P(4)	161.4(2)	C(204)–P(4)–C(411)	103.8(8)
W(1)–P(1)–C(103)	107.8(6)	C(204)–P(4)–C(421)	102.8(7)
W(1)–P(1)–C(111)	110.4(5)	C(411)–P(4)–C(421)	99.6(6)

[a] Numbers in parentheses are estimated standard deviations in the least significant digit.

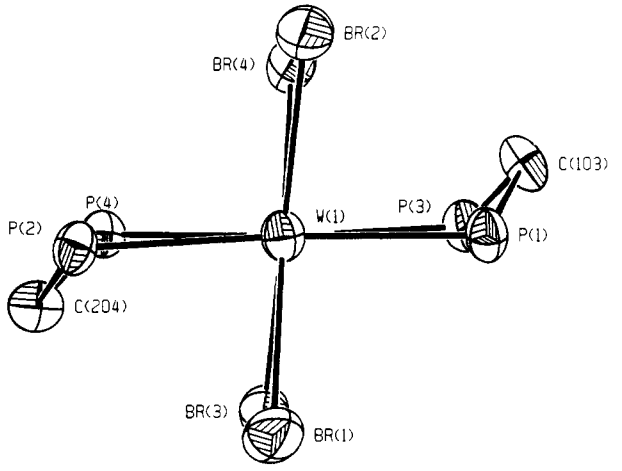

Figure 1. ORTEP drawing of the core of $W\equiv WBr_4(\mu\text{-dppm})_2$. Thermal ellipsoids are drawn at 50% probability.

WBr_5. It is also noteworthy that while WCl_4 and WBr_5 may be used in the direct synthesis of quadruply bonded complexes, there is no indication yet that quadruply bonded compounds can be synthesized directly from WCl_6.[6,17]

Synthesis of $W_2Br_4(PMe_2Ph)_4$ (5) and $W_2Br_4(PPh_2Me)_4$ (6). In contrast to the synthesis of **1**, the synthesis of the $W\equiv WBr_4$ core with monodentate phosphine ligands proceeds both in toluene at room temperature and at low temperatures in THF with $NaBEt_3H$ as the reducing agent. $W\equiv WBr_4L_4$ type complexes are quite sensitive to oxidation by dioxygen and to water. Evidence for this is found in the $^{31}P\{^1H\}$ NMR spectra of **5** and **6** which show significant amounts of $WOBr_2L_3$.[18] Mixtures of $W\equiv WBr_4L_4$ and $WOBr_2L_3$ are very difficult to separate, and the presence of $WOBr_2L_3$, indicated in the $^{31}P\{^1H\}$ NMR spectra, may retard the formation of crystalline $W\equiv WBr_4L_4$. The presence of such bulky phosphine and halide ligands may cause phosphine exchange or dissociation in solution and contribute to the difficulties in obtaining a crystal suitable for X-ray diffraction studies. Evidence for this behavior has been observed in the $^{31}P\{^1H\}$ NMR spectra. The use of a smaller phosphine ligand such as PMe_3 is being investigated.

Synthesis of $Mo\equiv WBr_4(PMe_2Ph)_4$ (2) and $Mo\equiv WBr_4(PPh_2Me)_4$ (7). The syntheses of $Mo\equiv WBr_4(PMe_2Ph)_4$ and $Mo\equiv WBr_4(PPh_2Me)_4$[8,19] are similar to those of $Mo\equiv WCl_4(PMe_2Ph)_4$ and $Mo\equiv WCl_4(PPh_2Me)_4$ except for the use of $WBr_4(PPh_3)_2$ instead of $WCl_4(PPh_3)_2$.[11] Through ligand ex-

Table IV. Positional and Thermal Parameters for Non-Hydrogen Atoms of $Mo\equiv WBr_4(PMe_2Ph)_4$

atom	*x*	*y*	*z*	*B*,[a] Å^2
MW(1)[b]	0.02065(4)	0.02359(2)	0.000	1.72(1)
Br(1)	–0.0463(1)	0.05412(4)	–0.1876(2)	3.20(4)
Br(2)	0.1152(1)	0.02617(4)	0.1957(2)	2.99(4)
P(1)	0.1254(3)	0.0232(1)	–0.1711(6)	2.8(1)
P(2)	–0.0617(2)	0.0540(1)	0.1653(5)	2.41(9)
C(11)	0.107(1)	0.0173(5)	–0.357(2)	4.6(5)
C(13)	0.202(1)	–0.0016(4)	–0.140(3)	4.9(5)
C(21)	–0.053(1)	0.0479(4)	0.349(2)	3.8(4)
C(23)	–0.1587(9)	0.0524(4)	0.142(2)	3.5(4)
C(121)	0.1656(7)	0.0613(3)	–0.166(1)	3.0(4)
C(122)	0.2119(7)	0.0692(3)	–0.056(1)	4.6(5)
C(123)	0.2400(7)	0.0986(3)	–0.047(1)	5.3(5)
C(124)	0.2220(7)	0.1201(3)	–0.149(1)	6.5(7)
C(125)	0.1758(7)	0.1121(3)	–0.259(1)	5.8(6)
C(126)	0.1476(7)	0.0827(3)	–0.267(1)	6.0(7)
C(221)	–0.0408(5)	0.0944(2)	0.0140(2)	3.0(4)
C(222)	0.0317(5)	0.1025(2)	0.116(2)	4.6(5)
C(223)	0.0497(15)	0.1328(2)	0.089(2)	6.2(7)
C(224)	–0.0049(5)	0.1549(2)	0.086(2)	5.6(6)
C(225)	–0.0774(5)	0.1467(2)	0.110(2)	6.8(7)
C(226)	–0.0954(5)	0.1165(2)	0.137(2)	5.4(6)

[a] Anisotropically refined atoms are given in the form of the equivalent isotropic displacement parameter defined as $^1/_3[a^2a^{*2}B_1 + b^2b^{*2}B_{22} + c^2c^{*2}B_{33} + 2ab(\cos\gamma)a^*b^*B_{12} + 2ac(\cos\beta)a^*c^*B_{13} + 2bc(\cos\alpha)b^*c^*B_{23}]$. [b] Hydrid metal atom composed of 53.8(7)% Mo and 46.2(7)% W.

Table V. Selected Bond Lengths (Å) and Angles (deg) for $Mo\equiv WBr_4(PMe_2Ph)_4$[a]

Bond Lengths			
MW(1)[b]–MW(1)	2.209(1)	P(1)–C(13)	1.79(2)
MW(1)–Br(1)	2.555(2)	P(1)–C(121)	1.83(1)
MW(1)–Br(2)	2.553(2)	P(2)–C(21)	1.79(2)
MW(1)–P(1)	2.523(5)	P(2)–C(23)	1.79(2)
MW(1)–P(2)	2.563(5)	P(2)–C(221)	1.83(1)
P(1)–C(11)	1.82(2)		
Bond Angles			
MW(1)–MW(1)–Br(1)	109.23(5)	MW(1)–P(1)–C(13)	119.3(9)
MW(1)–MW(1)–Br(2)	105.91(5)	MW(1)–P(1)–C(121)	106.3(4)
MW(1)–MW(1)–P(1)	104.7(1)	C(11)–P(1)–C(13)	102(2)
MW(1)–MW(1)–P(2)	106.8(1)	C(11)–P(1)–C(121)	103.3(8)
Br(1)–MW(1)–Br(2)	144.82(7)	C(13)–P(1)–C(121)	103.8(7)
Br(1)–MW(1)–P(1)	85.0(1)	MW(1)–P(2)–C(21)	118.3(6)
Br(1)–MW(1)–P(2)	82.9(1)	MW(1)–P(2)–C(23)	119.1(7)
Br(2)–MW(1)–P(1)	87.7(1)	MW(1)–P(2)–C(221)	107.5(5)
Br(2)–MW(1)–P(2)	85.6(1)	C(21)–P(2)–C(23)	102(1)
P(1)–MW(1)–P(2)	148.4(1)	C(21)–P(2)–C(221)	105.0(8)
MW(1)–P(1)–C(11)	119.7(8)	C(23)–P(2)–C(221)	103.3(7)

[a] Numbers in parentheses are estimated standard deviations in the least significant digit. [b] Hybrid metal atom composed of 53.8(7)% Mo and 46.2(7)% W.

(17) Agaskar, P. A.; Cotton, F. A.; Dunbar, K. R.; Falvello, L. R.; O'Connor, C. J. *Inorg. Chem.* **1987**, *26*, 4051.

(18) Cotton, F. A.; Mandel, S. K. *Inorg. Chim. Acta* **1992**, *194*, 179.

(19) Cotton, F. A.; Favello, L. R.; Luck, R. L.; James, C. A. *Inorg. Chem.* **1990**, *29*, 4759.

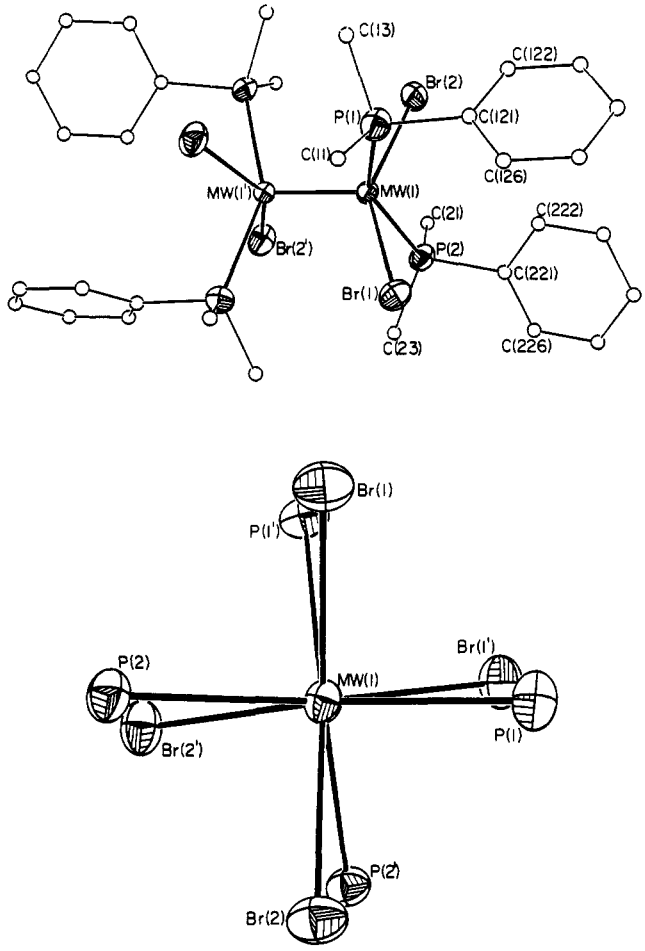

Figure 2. ORTEP drawings of the complete molecular geometry of $Mo\equiv WBr_4(PMe_2Ph)_4$ (top) and the central portion viewed down the Mo–W axis (bottom). Thermal ellipsoids, except for carbon atoms, are drawn at 50% probability.

change reactions, the compounds $Mo\equiv WBr_4(PMe_2Ph)_4$ and $Mo\equiv WBr_4(PPh_2Me)_4$ become versatile starting materials in the synthesis of other $Mo\equiv WBr_4L_4$ and $Mo\equiv WBr_4(L\text{-}L)_4$ compounds. The variable temperature $^{31}P\{^1H\}$ NMR spectra of these compounds are complex, but the behavior is similar to that of the $W\equiv WBr_4$ analogs.

Structure and Bonding. Compound 1. The structure of $W\equiv WBr_4(\mu\text{-dppm})_2$, shown in Figure 1, is of interest because it is the first example of a quadruply bonded ditungsten complex containing the $W\equiv WBr_4$ core. Its most interesting feature is the eclipsed geometry since the $W\equiv WCl_4(\mu\text{-dppm})_2$ complex has a torsional angle of 17.25°.[5] In this respect, **1** more closely resembles the dimolybdenum series $Mo\equiv MoX_4(\mu\text{-dppm})_2$, where X = Cl, Br, and I,[4,12,20-22] which all have an eclipsed geometry. The Mo≡Mo bond distances in $Mo\equiv MoCl_4(\mu\text{-dppm})_2$, $Mo\equiv MoBr_4(\mu\text{-dppm})_2$, and $Mo\equiv MoI_4(\mu\text{-dppm})_2$ are essentially identical, viz. 2.138(1) Å, 2.138(1) Å, and 2.139(1) Å, respectively, and the W≡W bond distance in $W\equiv WBr_4(\mu\text{-dppm})_2$ (2.2632(9) Å) is only slightly shorter than the bond distance in $W\equiv WCl_4(\mu\text{-dppm})_2$ (2.269(1) Å).[5] The slightly longer W≡W bond distance in $W\equiv WCl_4(\mu\text{-dppm})_2$ is probably attributable to the torsion angle.

(20) Abbott, E. H.; Bose, K. S.; Cotton, F. A.; Hall, W. T.; Sekutowski, J. C. *Inorg. Chem.* **1978**, *17*, 3240.
(21) Campbell, F. L.; Cotton, F. A.; Powell, G. L. *Inorg. Chem.* **1985**, *24*, 177.
(22) Bronikowski, M. J.; Dallinger, R. F.; Hopkins, M. D.; Gray, H. B.; Miskowski, V. M.; Schaefer, W. P.; Woodruff, W. H. *J. Am. Chem. Soc.* **1987**, *109*, 408.

Table VI. Selected Torsional Angles (deg) for $Mo\equiv WBr_4(PMe_2Ph)_4$[a]

Br(1)–MW(1)[b]–MW(1)'–P(1)'	−5.95(13)
Br(2)–MW(1)–MW(1)'–P(3)'	−9.54(12)
P(1)–MW(1)–MW(1)'–Br(1)'	−5.95(13)
P(3)–MW(1)–MW(1)'–Br(2)'	−9.54(12)

[a] Numbers in parentheses are estimated standard deviations in the least significant digit. [b] Hybrid metal atom composed of 53.8 (7)% Mo and 46.2 (7)% W.

The average W–X distances for the complexes $W\equiv WCl_4(\mu\text{-dppm})_2$ and $W\equiv WBr_4(\mu\text{-dppm})_2$ are 2.376 and 2.518 Å, respectively. The 0.14-Å increase in the W–X bond length is in agreement with the corresponding difference between the covalent radii of the two halides (0.15 Å). The same increase (0.14 Å) is observed in both the Mo–X and W–X bond lengths upon changing the halide from chloride to bromide, since in the analogous molybdenum system, the Mo–X distance increases from 2.394 to 2.535 Å.[22]

Compound 2. Although $Mo\equiv WBr_4(PMe_2Ph)_4$ contains a $MoWBr_4$ core, the structural characteristics of **2** are very similar to those of $Mo\equiv WCl_4(PMe_2Ph)_4$. The metal–metal bond distance of 2.209(1) Å is slightly longer than that of $Mo\equiv WCl_4(PMe_2Ph)_4$, 2.2007(4) Å. The only significant differences are in the M–X distance, which is 0.10 Å longer in the bromide complex, and in the M–M–X and M–M–P angles, which are slightly more obtuse for the bromide complex. Such structural changes are expected when changing the halide from Cl to Br, have been reported for the $Mo\equiv MoX_4(PMe_3)_4$ series,[22] and were also observed in the ditungsten complex reported here. One of the more interesting structural features is a notable twist between the two ends of the molecule shown in Figure 2. The average torsional angle of 7.75° was calculated from the individual angles listed in Table VI. This twist is probably due to the steric crowding caused by the interaction of the large bromide and phosphine ligands and may cause the slight lengthening of the $Mo\equiv WBr_4(PMe_2Ph)_4$ bond relative to that of $Mo\equiv WCl_4(PMe_2Ph)_4$. To our knowledge, there are no other examples of a $M\equiv M'X_4L_4$ type complex with a twisted configuration.

Spectroscopy. $^{31}P\{^1H\}$ NMR Spectroscopy. The $^{31}P\{^1H\}$ NMR spectra of both **1** and **2** are very similar to those of their chloride analogs except for the expected halide effects. The most important difference between the spectrum of $W\equiv WCl_4(\mu\text{-dppm})_2$ and that of $W\equiv WBr_4(\mu\text{-dppm})_2$ is an upfield shift due to the change in halide (Cl to Br). Since all the phosphorus atoms of the dppm ligands are equivalent, the $^{31}P\{^1H\}$ NMR spectrum of $W\equiv WBr_4(\mu\text{-dppm})_2$ is a singlet. At room temperature, the chemical shift for $W\equiv WCl_4(\mu\text{-dppm})_2$ is δ 18.15 ppm, while the chemical shift for $W\equiv WBr_4(\mu\text{-dppm})_2$ is δ 15.83 ppm. A similar trend is observed in the analogous dimolybdenum complexes, where $Mo\equiv MoCl_4(\mu\text{-dppm})_2$, $Mo\equiv MoBr_4(\mu\text{-dppm})_2$, and $Mo\equiv MoI_4(\mu\text{-dppm})_2$ have chemical shift values of δ 16.04 ppm, δ 14.87 ppm, and δ 12.04 ppm, respectively.

For $W\equiv WBr_4(PMe_2Ph)_4$ and $W\equiv WBr_4(PPh_2Me)_4$, the four phosphorus atoms are again equivalent, and there is a broad singlet for each of the compounds. The analogous chloride complexes, $W\equiv WCl_4(PMe_2Ph)_4$ and $W\equiv WCl_4(PPh_2Me)_4$, have reported chemical shifts of δ −1 ppm and δ 2 ppm, respectively.[6] However, both the chemical shifts and $\Delta\nu_{1/2}$ for complexes **5** and **6** are temperature dependent. For example, in $W\equiv WBr_4(PMe_2Ph)_4$ the chemical shift is δ −4.55 ppm ($\Delta\nu_{1/2}$ = 28.51 Hz) at −80 °C. As the temperature is increased to −20 °C, the chemical shift undergoes an upfield shift to δ −5.63 ppm and the line narrows ($\Delta\nu_{1/2}$ = 13.67 Hz). The chemical shift of $W_2Br_4(PPh_2Me)_4$ occurs at δ 1.25 ppm at −100 °C, and as the temperature is increased, the line broadens and the peak shifts upfield. The lines are so broad that no tungsten satellites are observed for either complex.

The origin of the temperature dependent behavior of the chemical shift in **5** and **6** is unknown, but there are several factors that may contribute. The bulky phosphine and bromide ligands may cause steric interactions in the complex. In solution, the phosphorus ligands may undergo exchange or dissociation causing an upfield shift of the observed chemical shift toward the chemical shift of free phosphine. Although the crystal structures of **5** and **6** are not known, the structure of the Mo–W analog **2** has been determined and has a small torsional angle. The presence of a torsional angle causes paramagnetism that is manifested in temperature dependent behavior of the $^{31}P\{^1H\}$ NMR chemical shift.[23]

For the A_2B_2X spin system of **2**, $Mo\equiv WBr_4(PMe_2Ph)_4$, at room temperature, the two sets of triplets occur at δ 11.3 ppm (W–P) and δ –24.0 ppm (Mo–P) with J_{P-P} = 22 Hz and J_{P-W} = 228.5 ppm. The temperature dependent behavior of the chemical shifts is analogous to that observed for **5** and **6**. At –100 °C the chemical shifts of the compound occur at δ 13.93 ppm (W–P) and –19.29 ppm (Mo–P). As the temperature is increased, the chemical shift of the phosphorus atoms bound to the molybdenum center of $Mo\equiv WBr_4(PMe_2Ph)_4$ moves upfield and $\Delta\nu_{1/2}$ increases from 53.07 Hz at –100 °C to a maximum of 171.37 Hz at –20 °C and then decreases to $\Delta\nu_{1/2}$ = 41.91 Hz at 50 °C. The same trend is observed for the phosphorus atoms bound to the tungsten center. In the analogous chloride compound $Mo\equiv WCl_4(PMe_2Ph)_4$, the two sets of triplets occur at δ 17.9 ppm and δ –19.5 ppm, but the temperature dependence, if any, has not been reported.[19]

For $Mo\equiv WBr_4(PPh_2Me)_4$, (**7**), the two sets of triplets occur at δ 16.57 ppm (W–P) and δ –16.63 ppm (Mo–P) with J_{P-P} = 22.7 Hz at –100 °C. The lines are broad, and no tungsten satellites are observed. The behavior of the chemical shifts with temperature is similar to that described previously for **2** and **5**. However, as the temperature is increased, the spectra become complex and additional peaks appear, due, presumably, to exchange or dissociation processes. The expected shift is observed owing to the change in halide from chloride to bromide (for the chloro analog of **7** the data are δ 17.4 ppm (W–P) and –20.1 ppm (M–P) J_{P-P} = 24.0 Hz).[24]

Diamagnetic Anisotropy of the $W\equiv WBr_4(\mu\text{-dppm})_2$ Bond. The chemical shift difference observed in the ^1H NMR spectrum for certain protons and their positions as calculated from the X-ray crystal structure data for complex **1** can be used to estimate the diamagnetic anisotropy of the tungsten–tungsten quadruple bond. For $W\equiv WCl_4(\mu\text{-dppm})_2$, $W\equiv WBr_4(\mu\text{-dppm})_2$, and $\alpha\text{-}W\equiv WCl_4(dppe)_2$, the methods and reference frame of Cotton and Chen[25] have been used to estimate $\Delta\chi$ using eq 1.

$$\Delta\delta = \frac{\Delta\chi}{4\pi}\left[\frac{1-3\cos^2\theta}{3r^3}\right] = \frac{\Delta\chi}{4\pi}G \qquad (1)$$

Here $\Delta\delta$ is the change in the chemical shift of the proton relative to the free ligand, r is the distance of the test nucleus from the center of the W≡W bond, and θ is the angle between the r vector and the W–W axis. Table VII contains the observed $\Delta\delta$'s, G factors, and the calculated $\Delta\chi$ for $W\equiv WCl_4(\mu\text{-dppm})_2$, $W\equiv WBr_4(\mu\text{-dppm})_2$, and $\alpha\text{-}W\equiv WCl_4(dppe)_2$. Estimates of $\Delta\chi$ made using this method contain ambiguities concerning the portion of $\Delta\delta$ which is actually due to $\Delta\chi$ and the portions which may be due to ring current effects of nearby phenyl rings or inductive effects resulting from the phosphorus binding to the metal center. Using the values of $\Delta\chi$ for the three complexes, an average value of -5728×10^{-36} m^3 molecule^{-1} is obtained for the diamagnetic anisotropy of the W≡W bond. For comparison,

Table VII. Diamagnetic Anisotropy for $W_2X_4(L\text{-}L)_2$ Complexes

compound		δ, ppm	r, Å	G,[a] m^3	$10^{36}\Delta\chi_{av}$
$W\equiv WCl_4(\mu\text{-dppm})_2$	H_1	2.2	4.47	1.05×10^{28}	–5596
	H_2	2.2	3.24	2.25×10^{28}	
$W\equiv WBr_4(\mu\text{-dppm})_2$	H_1	2.25	3.45	2.44×10^{28}	–5372
	H_2	2.25	4.35	1.22×10^{28}	
	H_3	2.25	3.55	2.23×10^{28}	
	H_4	2.25	4.40	1.17×10^{27}	
$\alpha\text{-}W\equiv WCl_4(dppe)_2$	H_1	2.9	3.48	2.36×10^{28}	–6213
	H_2	1.4	4.51	9.42×10^{27}	
	H_3	2.9	3.78	1.85×10^{28}	
	H_4	1.4	4.67	6.07×10^{27}	

[a] $G = (1-3\cos^2\theta)/3r^3$.

Table VIII. $^1\delta^2 \rightarrow {}^1(\delta\delta^*)$ Absorptions for $M\equiv MX_4P_4$ Compounds

	$^1\delta^2 \rightarrow {}^1(\delta\delta^*)$ abs band, nm		
X_4P_4	Mo≡Mo	Mo≡W	W≡W
$Cl_4(PMe_2Ph)_4$	593[28]	647[19]	674
$Cl_4(PPh_2Me)_4$	600[28]	650[8]	683
$Br_4(PMe_2Ph)_4$	614	666	682
$Br_4(PPh_2Me)_4$	623	670	689

an average value of -6500×10^{-36} m^3 molecule^{-1} has been reported for the Mo≡Mo bond and -5083×10^{-36} m^3 molecule^{-1} for the Mo≡W bond.[25,26] A value of -3000×10^{-36} m^3 molecule^{-1} previously estimated for W≡W[15] is unrealistically low compared to values for the dimolybdenum systems reported in the literature and values we have now determined for W≡W. While it is difficult to be sure, the method used to obtain it seems flawed.

It is well-known that heteronuclear organic bonds such as C=O and N=O have larger anisotropies than analogous homonuclear bonds C=C.[27] In light of this fact, one might not have been surprised to find the Mo≡W bond having a larger anisotropy than either the Mo≡Mo or W≡W bonds. However, there is little difference in the anisotropies of the Mo≡W, Mo≡Mo, and W≡W bonds.

UV–Vis Spectroscopy. The lowest energy electronic absorption band in the solution-state visible spectrum of $W\equiv WBr_4(\mu\text{-dppm})_2$, at 720 nm, can be assigned to the $^1\delta^2 \rightarrow {}^1(\delta\delta^*)$ transition. In $W\equiv WCl_4(\mu\text{-dppm})_2$, the band assigned to this transition occurs at 737 nm.[5] For the dimolybdenum system, the $^1\delta^2 \rightarrow {}^1(\delta\delta^*)$ transitions of the chloride, bromide and iodide analogs occur at 641, 654, and 709 nm respectively.[4] However, there are no torsion angles in either the dimolybdenum compounds or $W\equiv WBr_4(\mu\text{-dppm})_2$.[4,12,20] The torsion angle of 17.25° in $W\equiv WCl_4(\mu\text{-dppm})_2$ accounts for the slight blue shift (instead of a red shift) upon changing the halide from Cl to Br for $W\equiv WX_4(L\text{-}L)_2$.[5]

The $^1\delta^2 \rightarrow {}^1(\delta\delta^*)$ transitions for **2**–**7** are listed in Table VIII with those of other selected compounds for comparison. A red shift is consistently observed upon changing the halide from chloride to bromide, as has been previously noted for other $M\equiv M'X_4L_4$ compounds.[22] In $Mo\equiv Mo'X_4L_4$, $Mo\equiv W'X_4L_4$, and $W\equiv W'X_4L_4$ complexes, the red shifts are 22, 19.5, and 7 nm, respectively.

Acknowledgment. We are grateful to the National Science Foundation for Support and David J. Maloney for helpful discussions.

Supplementary Material Available: Fully numbered ORTEP drawing and full lists of crystallographic data and data collection parameters, bond distances, bond angles, anisotropic thermal parameters, and H atom positions (21 pages). Ordering information is given on any current masthead page.

(23) Campbell, G. C.; Haw, J. F. *Inorg. Chem.* **1988**, *27*, 3706.
(24) Cotton, F. A.; Luck, R. L.; James, C. A. *Inorg. Chem.* **1991**, *30*, 4370.
(25) Chen, J. D.; Cotton, F. A.; Falvello, L. R. *J. Am. Chem. Soc.* **1990**, *112*, 1076.
(26) Cotton, F. A.; James, C. J. *Inorg. Chem.* **1992**, *31*, 5298.
(27) Harris, R. K. *Nuclear Magnetic Resonance Spectroscopy*. Longman: Harlow, U.K. 1986.
(28) Cotton, F. A.; Daniels, L. M.; Powell, G. L.; Kahaian, A. J.; Smith, T. J.; Vogel, E. F. *Inorg. Chim. Acta* **1988**, *144*, 109.